

École Doctorale des Sciences de l'Environnement d'Île-de-France  
Année 2007-2008

Modélisation Numérique  
de l'Écoulement Atmosphérique  
et Assimilation d'Observations

Olivier Talagrand  
Cours 8  
13 Juin 2008

## Adjoint Approach

$$\mathcal{J}(\xi_0) = (1/2) (x_0^b - \xi_0)^T [P_0^b]^{-1} (x_0^b - \xi_0) + (1/2) \sum_k [y_k - H_k \xi_k]^T R_k^{-1} [y_k - H_k \xi_k]$$

subject to  $\xi_{k+1} = M_k \xi_k, \quad k = 0, \dots, K-1$

Control variable  $\xi_0 = u$

Adjoint equation

$$\lambda_K = H_K^T R_K^{-1} [H_K \xi_K - y_K]$$

$$\lambda_k = M_k^T \lambda_{k+1} + H_k^T R_k^{-1} [H_k \xi_k - y_k] \quad k = K-1, \dots, 1$$

$$\lambda_0 = M_0^T \lambda_1 + H_0^T R_0^{-1} [H_0 \xi_0 - y_0] + [P_0^b]^{-1} (\xi_0 - x_0^b)$$

$$\nabla_u \mathcal{J} = \lambda_0$$

Result of direct integration ( $\xi_k$ ), which appears in quadratic terms in expression of objective function, must be kept in memory from direct integration.

## Adjoint Approach (continued 2)

### Nonlinearities ?

$$\mathcal{J}(\xi_0) = (1/2) (x_0^b - \xi_0)^T [P_0^b]^{-1} (x_0^b - \xi_0) + (1/2) \sum_k [y_k - H_k(\xi_k)]^T R_k^{-1} [y_k - H_k(\xi_k)]$$

subject to  $\xi_{k+1} = M_k(\xi_k), \quad k = 0, \dots, K-1$

Control variable  $\xi_0 = u$

Adjoint equation

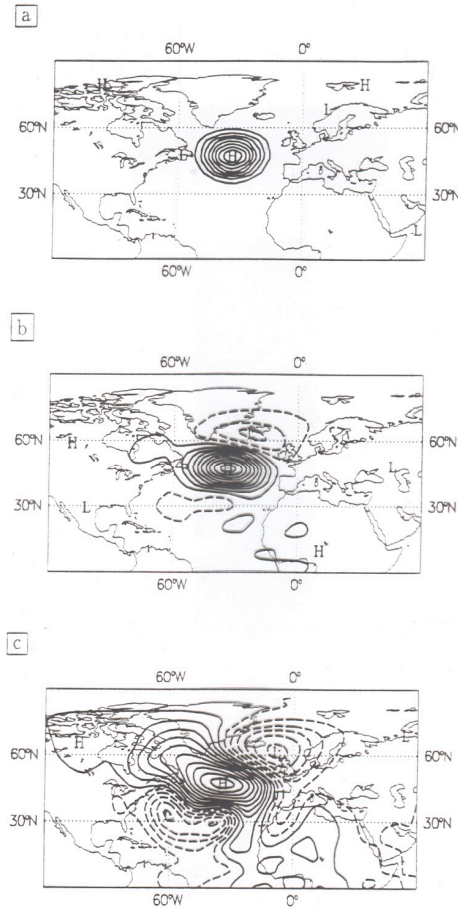
$$\lambda_K = H_K'^T R_K^{-1} [H_K(\xi_K) - y_K]$$

$$\lambda_k = M_k'^T \lambda_{k+1} + H_k'^T R_k^{-1} [H_k(\xi_k) - y_k] \quad k = K-1, \dots, 1$$

$$\lambda_0 = M_0'^T \lambda_1 + H_0'^T R_0^{-1} [H_0(\xi_0) - y_0] + [P_0^b]^{-1} (\xi_0 - x_0^b)$$

$$\nabla_u \mathcal{J} = \lambda_0$$

Not heuristic (it gives the exact gradient  $\nabla_u \mathcal{J}$ ), and really used as described here.



Temporal evolution of the 500-hPa geopotential autocorrelation with respect to point located at 45N, 35W. From top to bottom: initial time, 6- and 24-hour range. Contour interval 0.1. After F. Bouttier.

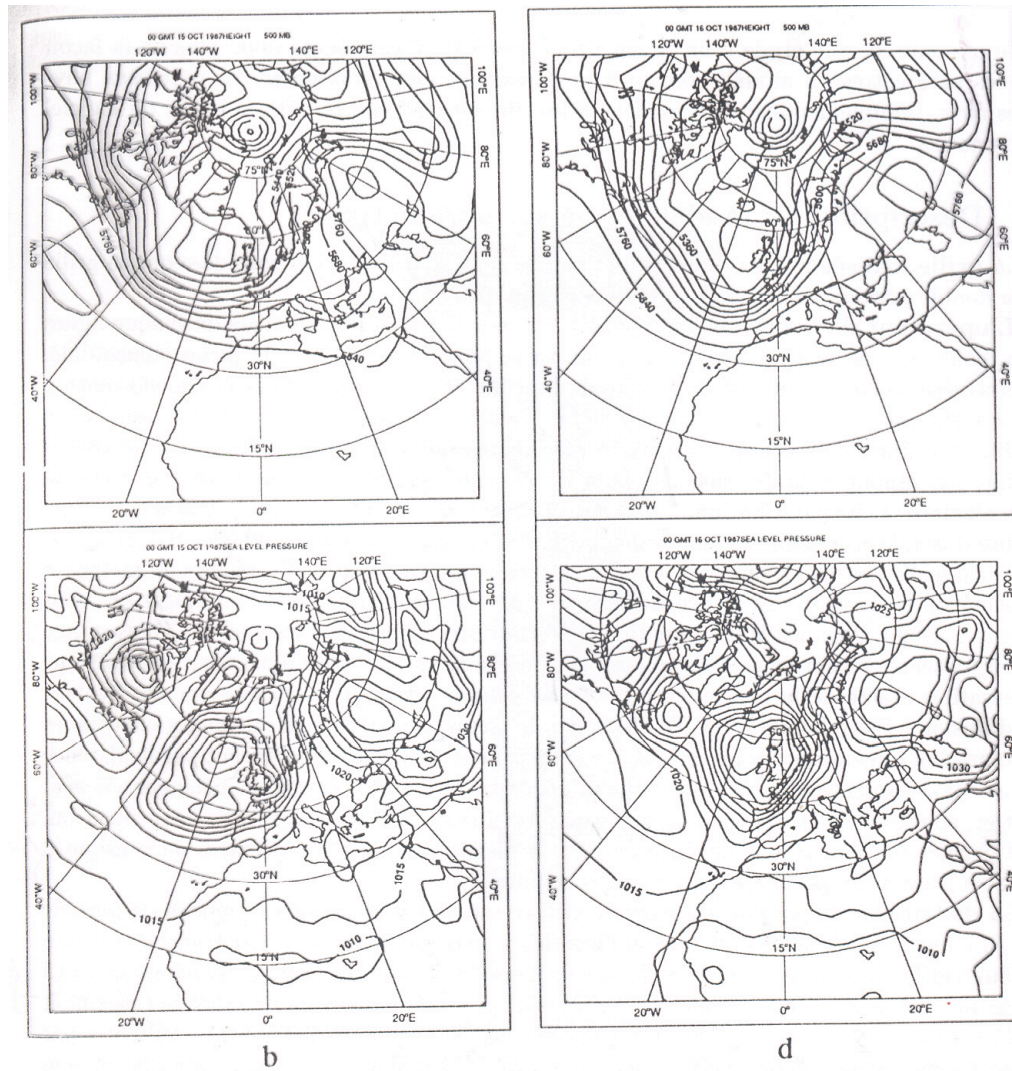
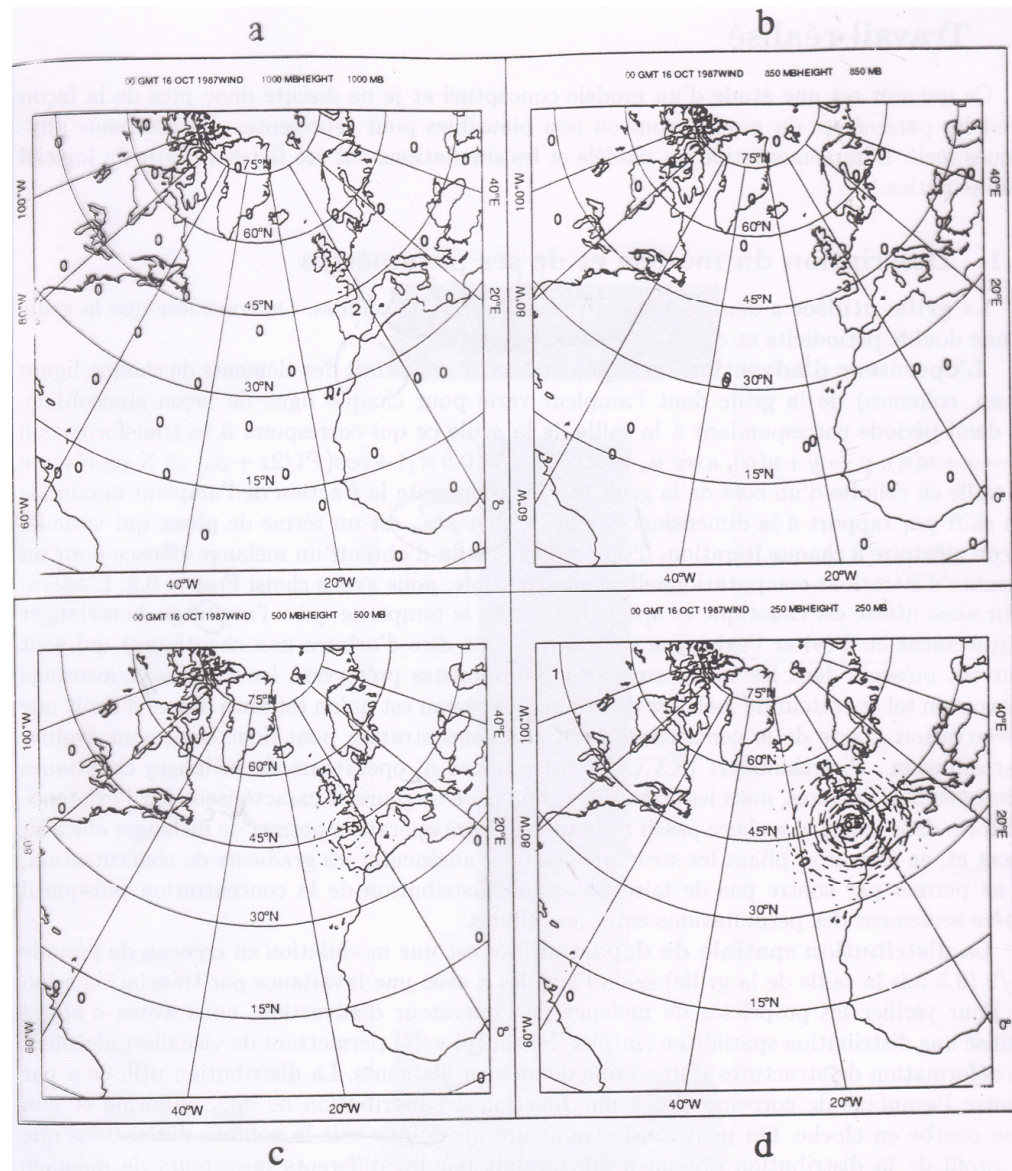
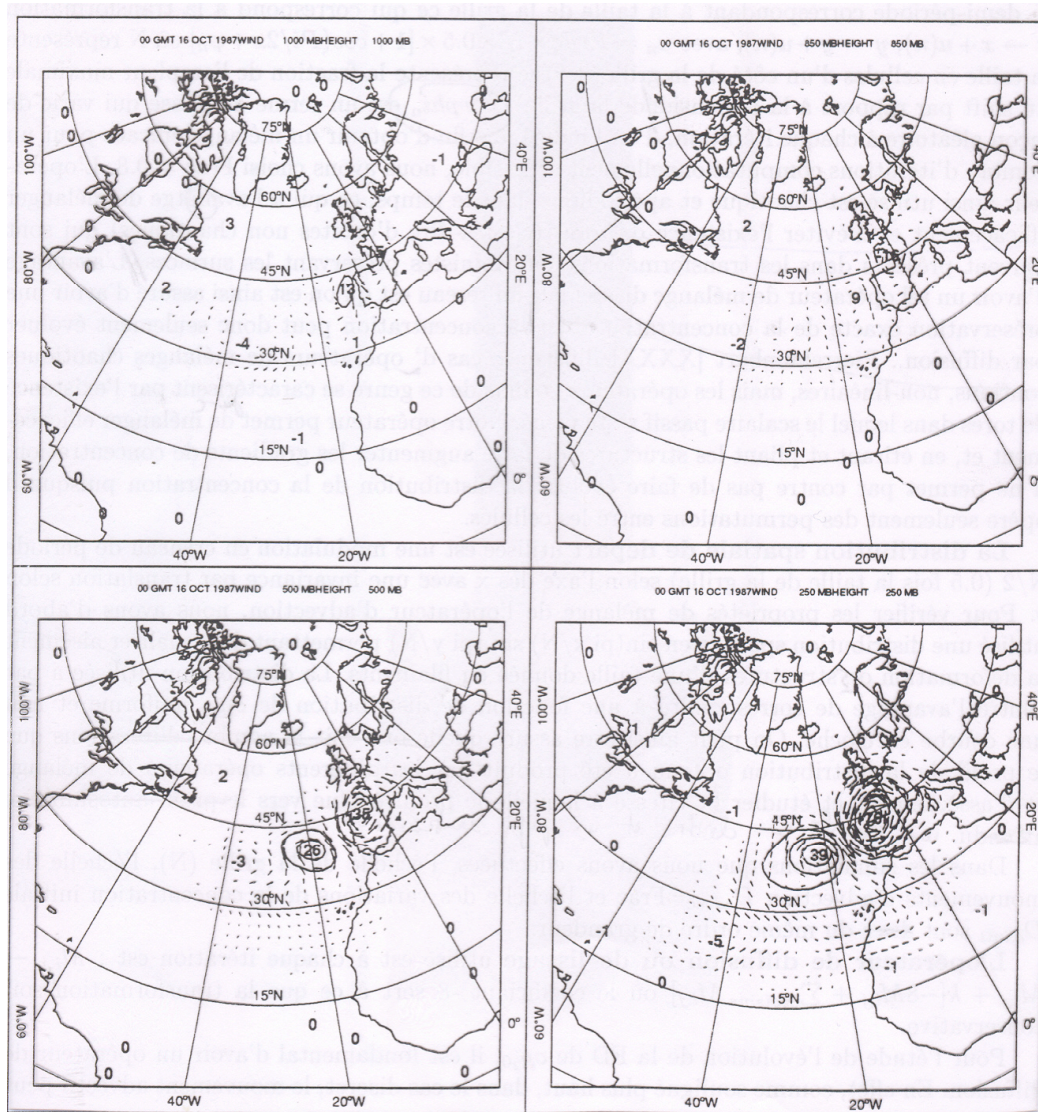


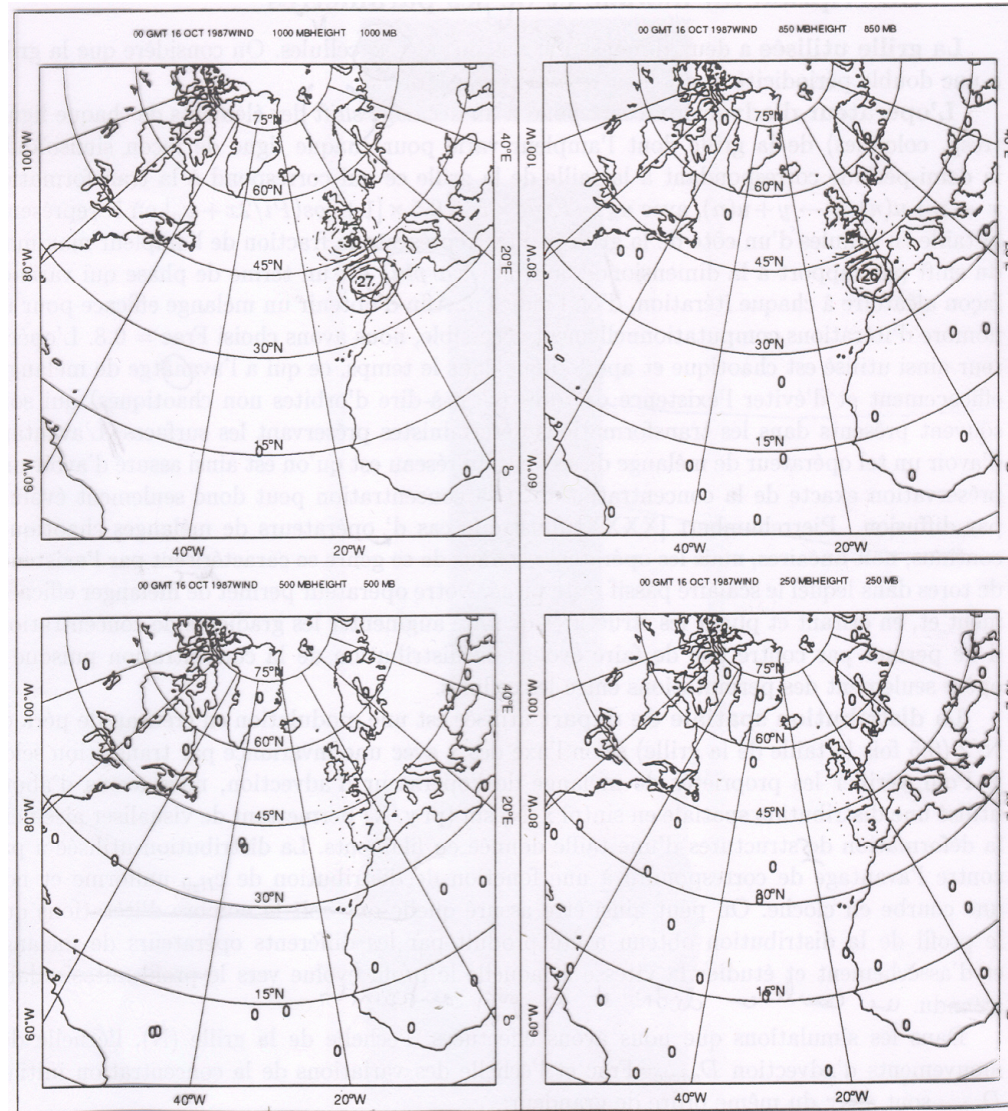
FIG. 1. Background fields for 0000 UTC 15 October–0000 UTC 16 October 1987. Shown here are the Northern Hemisphere (a) 500-hPa geopotential height and (b) mean sea level pressure for 15 October and the (c) 500-hPa geopotential height and (d) mean sea level pressure for 16 October. The fields for 15 October are from the initial estimate of the initial conditions for the 4DVAR minimization. The fields for 16 October are from the 24-h T63 adiabatic model forecast from the initial conditions. Contour intervals are 80 m and 5 hPa.



Analysis increments in a 3D-Var corresponding to a height observation at the 250-hPa pressure level (no temporal evolution of background error covariance matrix)



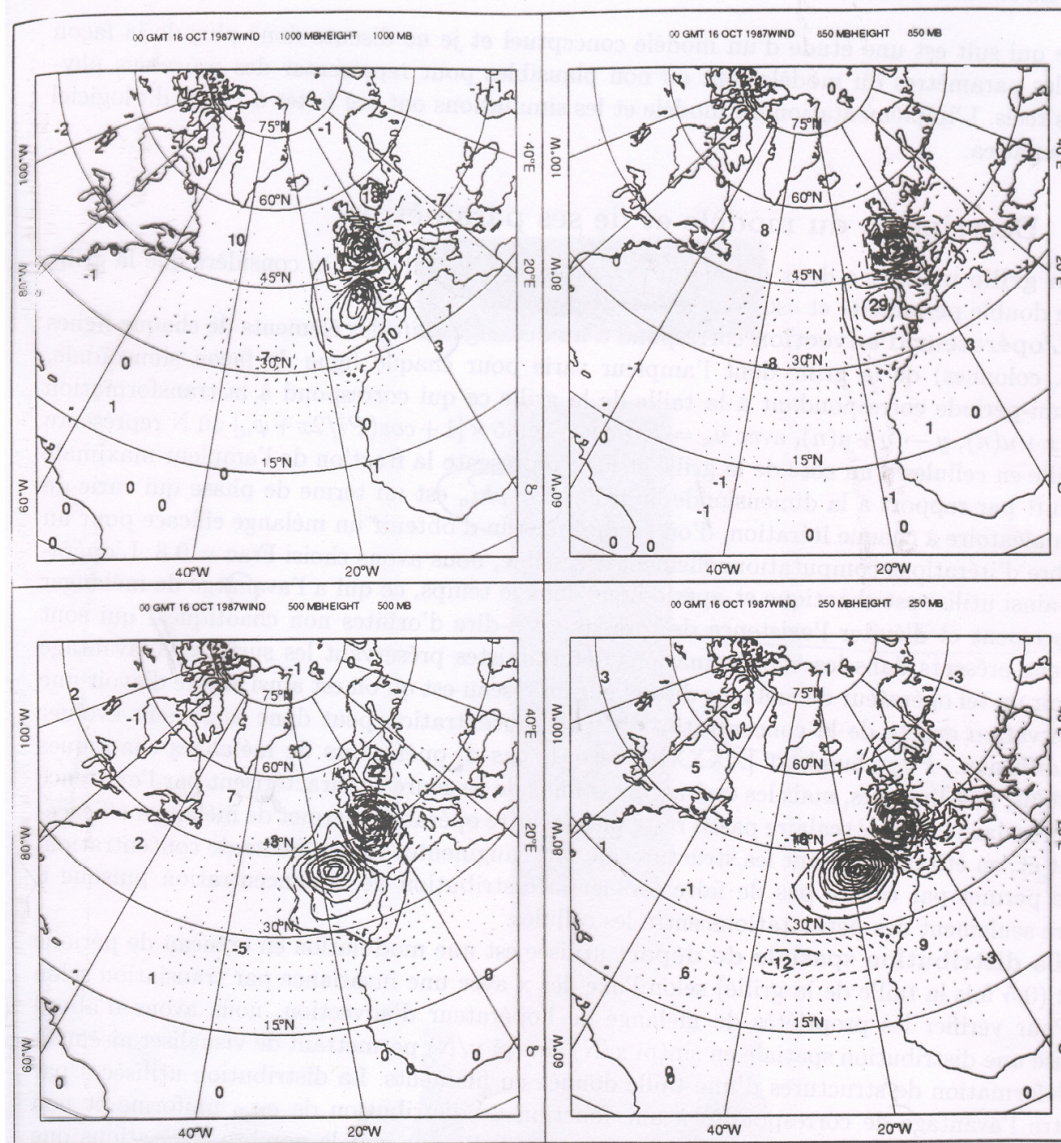
Same as before, but at the end of a 24-hr 4D-Var



Analysis increments in a 3D-Var corresponding to a  $u$ -component wind observation at the 1000-hPa pressure level (no temporal evolution of background error covariance matrix)

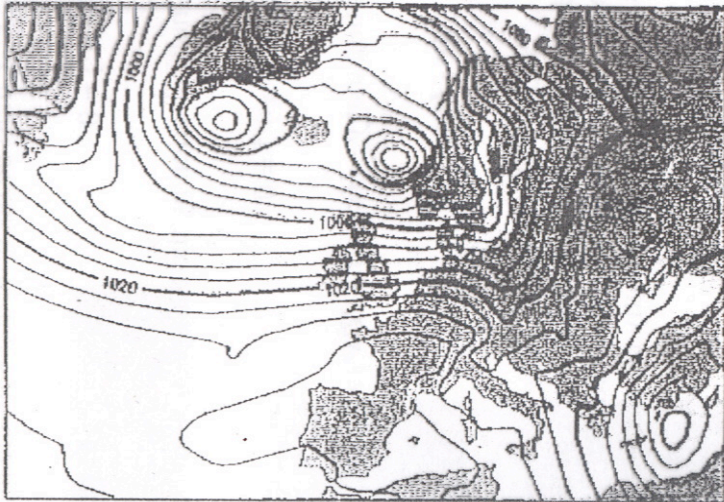
Thépaut *et al.*, 1993, *Mon. Wea. Rev.*, **121**, 3393-3414



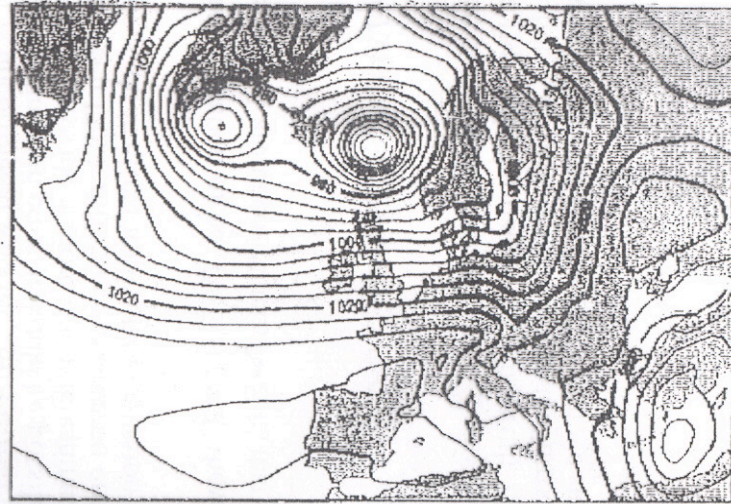


Same as before, but at the end of a 24-hr 4D-Var

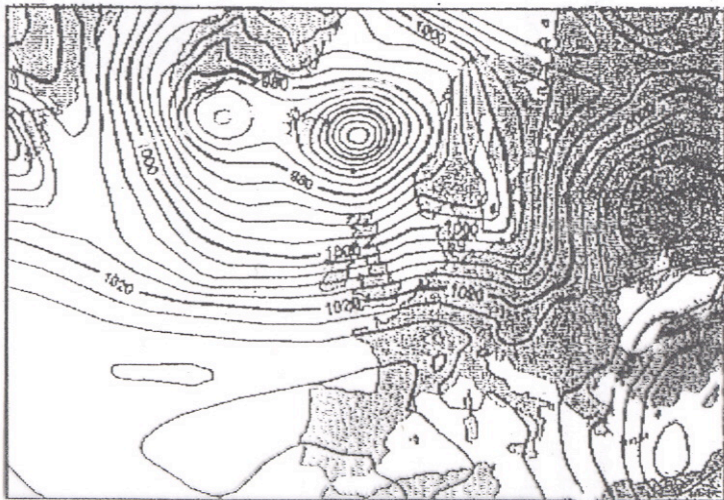
3-day forecast from 3D-Var analysis



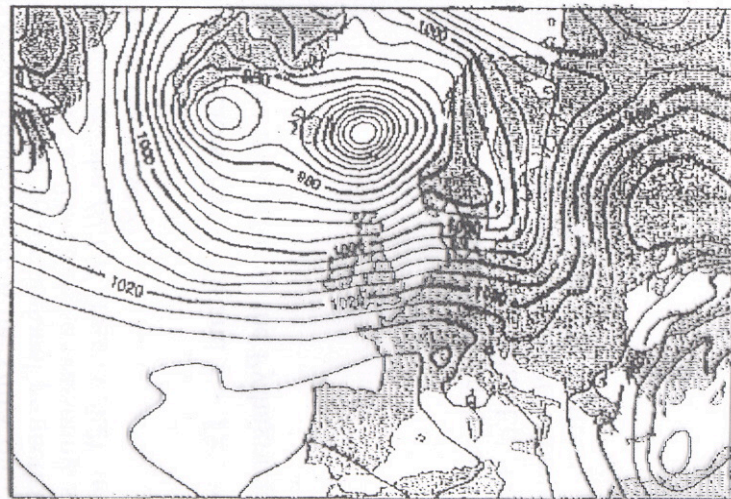
3-day forecast from 4D-Var analysis



3D-Var verifying analysis



4D-Var verifying analysis



ECMWF, Results on one FASTEX case (1997)

*4D-Var* is now used operationally at ECMWF, Météo-France, Meteorological Office (UK), Canadian Meteorological Service (together with an ensemble assimilation system), Japan Meteorological Agency

Model error is ignored

*Strong Constraint Variational Assimilation*